IOP PUBLISHING NANOTECHNOLOGY
Nanotechnology **24** (2013) 405102 (7pp) doi:10.1088/0957-4484/24/40/405102

# Liver-specific microRNAs as biomarkers of nanomaterial-induced liver damage

**Takashi Nagano[1,6], Kazuma Higashisaka[1,6], Akiyoshi Kunieda[1], Yuki Iwahara[1], Kota Tanaka[1], Kazuya Nagano[2], Yasuhiro Abe[3], Haruhiko Kamada[2,4], Shin-ichi Tsunoda[2,4], Hiromi Nabeshi[5], Tomoaki Yoshikawa[1], Yasuo Yoshioka[1,7] and Yasuo Tsutsumi[1,2,4,7]**

[1] Laboratory of Toxicology and Safety Science, Graduate School of Pharmaceutical Sciences, Osaka University, 1-6 Yamadaoka, Suita, Osaka 565-0871, Japan
[2] Laboratory of Biopharmaceutical Research, National Institute of Biomedical Innovation, 7-6-8, Saito-Asagi, Ibaraki, Osaka 567-0085, Japan
[3] Cancer Biology Research Center, Sanford Research/USD, Sioux Falls, SD, USA
[4] The Center for Advanced Medical Engineering and Informatics, Osaka University, 1-6, Yamadaoka, Suita, Osaka 565-0871, Japan
[5] Division of Foods, National Institute of Health Sciences, Tokyo, Japan

E-mail: yasuo@phs.osaka-u.ac.jp and ytsutsumi@phs.osaka-u.ac.jp

Received 9 May 2013, in final form 23 August 2013
Published 12 September 2013
Online at stacks.iop.org/Nano/24/405102

**Abstract**
Although nanomaterials are being used in various fields, their safety is not yet sufficiently understood. We have been attempting to establish a nanomaterials safety-assessment system by using biomarkers to predict nanomaterial-induced adverse biological effects. Here, we focused on microRNAs (miRNAs) because of their tissue-specific expression and high degree of stability in the blood. We previously showed that high intravenous doses of silica nanoparticles of 70 nm diameter (nSP70) induced liver damage in mice. In this study, we compared the effectiveness of serum levels of liver-specific or -enriched miRNAs (miR-122, miR-192, and miR-194) with that of conventional hepatic biomarkers (alanine aminotransferase (ALT) and aspartate aminotransferase (AST)) as biomarkers for nSP70. After mice had been treated with nSP70, their serum miRNAs levels were measured by using quantitative RT-PCR. Serum levels of miR-122 in nSP70-treated mice were the highest among the three miRNAs. The sensitivity of miR-122 for liver damage was at least as good as those of ALT and AST. Like ALT and AST, miR-122 may be a useful biomarker of nSP70. We believe that these findings will help in the establishment of a nanomaterials safety-assessment system.

## 1. Introduction

Nanomaterials are defined as substances that have at least one dimension less than 100 nm long. They are now widely used in cosmetics, foods, and medicines because they possess innovative functions such as high electrical conductivity, tensile strength, and tissue permeability [1, 2]. However, with the development of nanomaterials has come concern that, unlike the case with microsized materials, their unique characteristics may induce unexpected biological responses [3–5]. For example, recent reports have shown that carbon nanotubes can induce mesothelioma-like lesions in mice, similar to those induced by asbestos [6]. In addition, our group has shown that silica nanoparticles with a diameter of 70 nm (nSP70) can induce severe liver damage and pregnancy complications in mice, and reactive oxygen species (ROS) generation and DNA damage *in vitro*, whereas microsized silica particles do not have these effects [7–10]. Nevertheless, because nanomaterials have the potential to improve our quality of life, it is important that we develop and promote the use of safe forms. Furthermore, the development of

[6] These authors contributed equally to the work.
[7] Address for correspondence: Laboratory of Toxicology and Safety Science, Graduate School of Pharmaceutical Sciences, Osaka University, 1-6 Yamadaoka, Suita, Osaka 565-0871, Japan.

 

biomarkers of the biological effects of nanomaterials would be invaluable for establishing a nanomaterials safety-assessment system and strategies for the development, production, and use of safe forms of nanomaterials. We have already explored biomarkers, with a focus on proteins, and have shown that acute-phase proteins such as haptoglobin, serum amyloid A, and C-reactive protein could be useful biomarkers of the biological effects of silica or platinum nanoparticles [11–13]. However, the use of proteins alone is not sufficient for predicting the adverse biological effects of nanomaterials, as we need to evaluate biomarkers consisting of other biological molecules.

microRNAs (miRNAs) are highly conserved and small (18- to 25-nucleotide) RNAs that play pivotal roles in gene expression—specifically at the post-transcriptional level—in plants and animals. In humans, miRNAs are involved in the regulation of development, cell differentiation, proliferation, and apoptosis [14, 15], because they regulate as many as one-third of all messenger RNAs (mRNAs) [16, 17]. Furthermore, recent reports have demonstrated that miRNAs would serve as useful biomarkers for the non-invasive, tissue-specific evaluation of diseases and drug-induced tissue damage [18, 19]. This is because they show tissue-specific expression [20, 21] and exist in a stable form in the blood, saliva, and urine [22–24].

From this perspective, we focused on miRNAs as biomarkers for predicting the biological effects of nanomaterials. Although there have been some analyses of the changes in miRNA expression following exposure to nanomaterials [25, 26], there have been very few attempts to use miRNAs as biomarkers of nanomaterials. We therefore need to collect systematic information on miRNAs as biomarkers so as to predict nanomaterials-induced biological effects and thus establish a nanomaterials safety-assessment system.

In this study, as a first trial, we attempted to investigate whether liver-specific or -enriched miRNAs (miR-122, miR-192, and miR-194) could be used as reliable biomarkers for liver damage induced by nSP70.

## 2. Materials and methods

### *2.1. Materials*

Silica particles were purchased from micromod Partikeltechnologie (Rostock/Warnemünde, Germany). Silica particles with diameters of 70, 300, and 1000 nm (nSP70, nSP300, and mSP1000, respectively) were used. In addition, we used nSP70 modified with surface functional groups-a carboxyl group (nSP70-C) or an amino group (nSP70-N). The particles were sonicated for 5 min and then vortexed for 1 min before use. Lipopolysaccharide (LPS) and D-galactosamine hydrochloride (D-GalN) were purchased from Sigma-Aldrich (Tokyo, Japan).

### *2.2. Animals*

Female BALB/c mice were purchased from Nippon SLC, Inc. (Shizuoka, Japan) and used at 6–7 weeks of age. All of the animal experimental procedures were performed in accordance with the Osaka University and National Institute of Biomedical Innovation guidelines for the welfare of animals.

### *2.3. Blood sample collection*

BALB/c mice ($n = 5$ or 6 per group) were treated in various experiments with nSP70 at 10, 20, or 40 mg $kg^{-1}$ or with nSP70-C, nSP70-N, nSP300, or mSP1000 at 40 mg $kg^{-1}$, via injection into the tail vein. As positive control of induction of liver damage, BALB/c mice ($n = 5$ or 6 per group) were intraperitoneally treated with LPS at 10 $\mu$g $kg^{-1}$ and D-GalN at 700 mg $kg^{-1}$. Blood samples were collected at varying times (4, 8, 24, or 72 h after treatment) in several experiments. Sera were harvested by blood centrifugation at 8000*g* for 15 min.

### *2.4. Biochemical analysis*

Serum levels of alanine aminotransferase (ALT) and aspartate aminotransferase (AST) were measured with a DRI-CHEM 7000 biochemical analyzer (Fujifilm Corp., Tokyo, Japan).

### *2.5. Isolation of total RNA from serum*

We extracted total RNA, including small RNA, from serum samples by using a miRNeasy Mini Kit (QIAGEN, Tokyo, Japan) in accordance with the manufacturer's instructions. In brief, 250 $\mu$l of QIAzol lysis reagent was added to 50 $\mu$l of serum. After the addition of 50 $\mu$l of chloroform, the samples were mixed completely and centrifuged. Then, 100 $\mu$l of supernatant was transferred to a new tube and mixed with 150 $\mu$l of 100% ethanol. The sample was then applied directly to a RNeasy Mini spin column (QIAGEN) and the combined RNA to column was cleaned with wash buffers to remove impurities. Total RNA was eluted in 30 $\mu$l of RNase-free water.

### *2.6. Real-time quantitative reverse-transcription PCR (qRT-PCR)*

Serum levels of miR-122, miR-192, and miR-194 were measured by using TaqMan RT-PCR. Each miRNA in 5 $\mu$l of purified total RNA was reverse transcribed with a miRNA-specific stem-loop reverse transcriptase primer (Life Technologies, Tokyo, Japan). TaqMan RT-PCR was performed on a StepOne Plus real-time PCR system (Life Technologies, Tokyo, Japan). Generally, typical internal controls for miRNA expression, such as U6 RNA and 5S rRNA, are degraded in serum samples [27]. Therefore, we equalized all of the conditions and then normalized the levels of each miRNA by serum volume. The expression level of each miRNA is shown as a relative fold-change. Relative expression was compared between the silica-particle-treated group and the untreated group.

### *2.7. Statistical analyses*

All results are expressed as means ± SEM differences were compared by using the Student's *t*-test or Bonferroni test after ANOVA (analysis of variance).

## 3. Results

### *3.1. Physicochemical properties of silica nanoparticles*

Silica nanoparticles are common nanomaterials that are being used in cosmetics, foods, and medicines [28, 29]. Considering that further use of silica nanoparticles is expected, it is important to assess their safety. We used silica particles with diameters of 70 nm (nSP70), 300 nm (nSP300), and 1000 nm (mSP1000), as well as nSP70 with carboxyl (nSP70-C) or amino (nSP70-N) surface functional groups. In our previous study, we confirmed by transmission electron microscopy that all silica particles of the above-listed sizes and types were smooth-surfaced spheres [7–10]. We have already shown that the hydrodynamic diameters of nSP70, nSP70-C, nSP70-N, nSP300, and mSP1000 are 64.6, 69.6, 71.8, 322, and 1140 nm, respectively, and their zeta potentials (overall surface potentials) are −52.7, −76.3, −29.0, −62.1, and −67.0 mV, respectively [7–10]. The carboxyl and amino surface modifications therefore altered the surface charge of the nSP70 particles. In addition, we have already shown that the size-distribution spectrum of each set of silica particles had a single peak, and the measured hydrodynamic diameter corresponded almost precisely to the primary particle size of each set of silica particles [7–10]. These results indicated that the silica particles used in this study were well dispersed in solution.

### *3.2. Liver-specific or -enriched miRNAs as biomarkers of silica nanoparticles*

To evaluate the usefulness of microRNAs (miRNAs) as biomarkers for nanomaterials, we focused on a model of liver damage induced by nSP70. We have previously shown that treatment of mice with high-dose nSP70 intravenously via the tail vein induced lethal toxicity and severe liver damage. Therefore, we assessed the usefulness of the liver-specific or -enriched miRNAs miR-122, miR-192, and miR-194 as biomarkers of liver damage. miR-122 and miR-192 are the two miRNAs expressed most abundantly in the human liver [30], and hepatic miR-194 is highly expressed in hepatic epithelial cells, including hepatocytes, which are parenchymal cells and account for more than 80% of liver cells [31]. Therefore, to collect systematic information on whether miRNAs have the potential to be biomarkers of nanomaterials, we selected those three major miRNAs in liver. Mice were given nSP70, nSP300, or mSP1000 via the tail vein. A dose rate of 40 mg $kg^{-1}$ was chosen, because in the case of nSP70 this dose rate significantly increases the levels of ALT and AST [10]. As positive control, mice were intraperitoneally treated with LPS and D-GalN. At 8 h after treatment, we evaluated the serum level of each miRNA by using qRT-PCR and those of ALT and AST (i.e. the conventional hepatic biomarkers) by using biochemical analysis. The levels of miR-122 (figure 1(A)), ALT (figure 1(B)), and AST (figure 1(C)) in LPS/D-GalN-treated mice were significantly increased compared to those of vesicle-treated mice. The levels of miR-122 (figure 1(A)) and miR-192 (figure 1(D)) in nSP70-treated mice were significantly greater than those in saline-, nSP300- or mSP1000-treated mice and untreated mice. In contrast, the serum levels of miR-194 did not differ significantly among any groups (figure 1(E)). In addition, the levels of ALT (figure 1(B)) and AST (figure 1(C)) in nSP70-treated mice were significantly greater than those in saline-, nSP300- or mSP1000-treated mice and untreated mice. Thus, miR-122 and miR-192 may be useful as biomarkers for evaluating liver damage induced by nSP70. We focused on miR-122 in the following assessment, because it had the highest rate of expression among the three miRNAs.

### *3.3. Sensitivity and time-dependency of miR-122 expression*

To more precisely assess the serum levels of miR-122 as a biomarker, we examined the sensitivity and time-dependency of miR-122 expression after treatment with nSP70. Mice were intravenously treated with nSP70 at 10, 20, or 40 mg $kg^{-1}$. Blood samples were collected 8 h after treatment and the levels of miR-122, ALT, and AST were measured. The serum levels of miR-122 (figure 2(A)), ALT (figure 2(B)), and AST (figure 2(C)) showed dose-dependent patterns of expression. In mice treated with 40 mg $kg^{-1}$ nSP70 and 20 mg $kg^{-1}$ in the case of AST, the levels of all three markers were significantly greater than in untreated or saline-treated mice. Thus, as was the case with ALT and AST, the increase in serum miR-122 levels was dependent on the dose of nSP70. Next, to assess the time-dependency of miR-122 expression, we examined the serum levels of miR-122 (figure 2(D)), ALT (figure 2(E)), and AST (figure 2(F)) at 4, 8, 24, and 72 h after intravenous injection of nSP70 at 40 mg $kg^{-1}$. The serum levels of miR-122 in nSP70-treated mice were significantly higher than those in saline-treated mice at every time point, as was the case with ALT and AST. These results suggested that the pattern of release of miR-122 into the blood was the same as those of ALT and AST.

### *3.4. miR-122 response after treatment of mice with surface-modified nSP70*

Our group has previously demonstrated that modification of nSP70 with surface functional groups such as a carboxyl group (nSP70-C) or amino group (nSP70-N) can reduce the toxic effects of nSP70 (e.g., pregnancy complications in mice and ROS generation and DNA damage *in vitro*) [8, 9]. Here, we tested the use of miR-122 as a biomarker to determine whether the safety of nSP70 could be improved by adding functional groups. BALB/c mice were treated intravenously with nSP70, nSP70-C, or nSP70-N at 40 mg $kg^{-1}$. At 8 h after treatment, we measured the levels of miR-122 (figure 3(A)), ALT (figure 3(B)), and AST (figure 3(C)). The serum levels of miR-122 in nSP70-C- or nSP70-N-treated mice were significantly lower than that in nSP70-treated mice and were almost the same as those in untreated or saline-treated mice. The serum levels of ALT after treatment with nSP70-C or nSP70-N showed a trend similar to those of miR-122. In contrast, although the level of AST in nSP70-N-treated mice was significantly lower than that in nSP70-treated mice, the

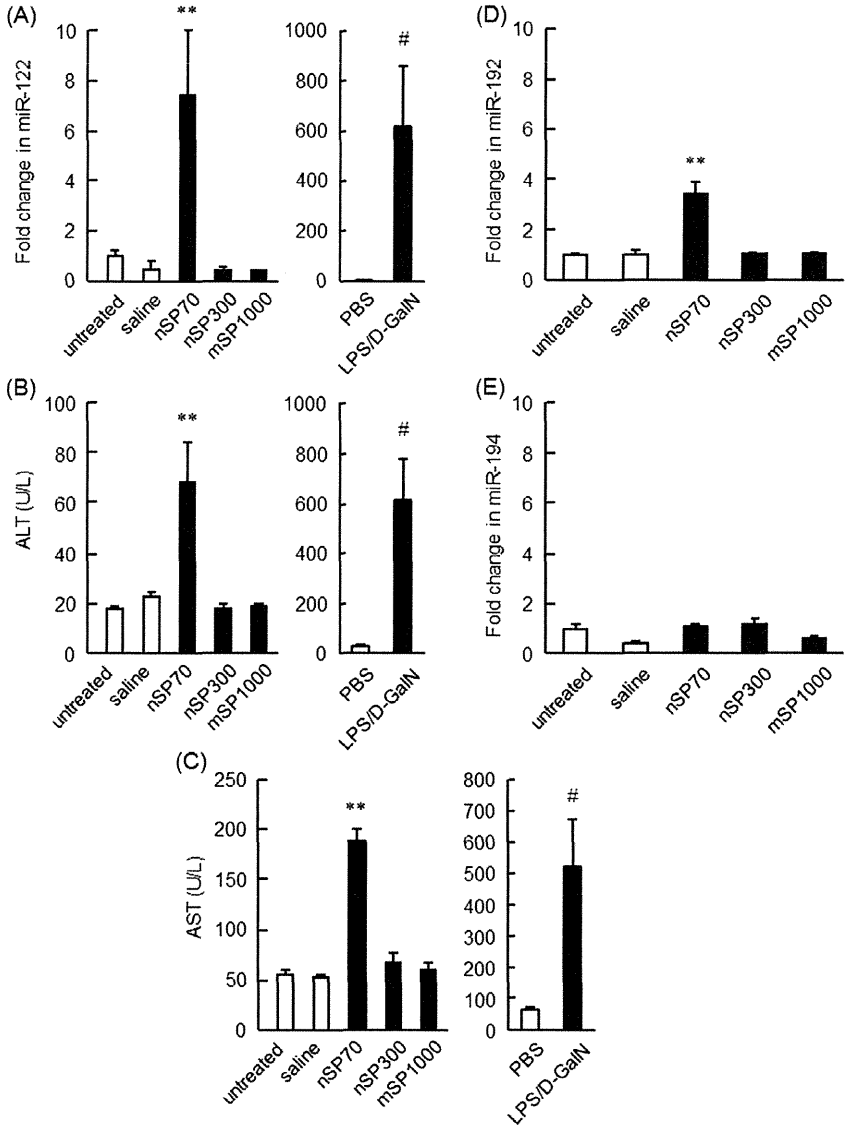


**Figure 1.** Usefulness of liver-specific microRNAs (miR-122, miR-192, and miR-194) as biomarkers for the development of safe silica nanoparticles. BALB/c mice were intravenously treated with nSP70, nSP300, or mSP1000 at 40 mg $kg^{-1}$. In addition, as positive control, mice were intraperitoneally treated with LPS and D-GalN. After 8 h, the serum levels of each microRNA, (A) miR-122, (D) miR-192, and (E) miR-194, were examined by real-time quantitative reverse-transcription PCR. Serum levels of (B) alanine aminotransferase (ALT) and (C) aspartate aminotransferase (AST) were measured by biochemical analysis. Data are presented as means ± SEM ($n = 6$; $^{**}P < 0.01$ versus value for saline-, nSP300-, mSP1000-treated group and untreated group by ANOVA; $^{\#}P < 0.05$ versus value for PBS-treated group by Student's *t*-test).

AST level in nSP70-C-treated mice was significantly greater than that in untreated or saline-treated mice. These results suggest that serum miR-122 may be useful as a biomarker for assessing improvement of the safety of nSP70 through surface modification.

## 4. Discussion

Our group showed previously that nSP70 can induce severe liver damage in mice [10]. Here, we examined whether liver-specific or -enriched miRNAs (miR-122, miR-192, and miR-194) were potentially useful as biomarkers of the liver damage induced by nSP70. Although miR-192 and miR-194 are thought to be involved in controlling proliferation and metastasis in liver cancer, the details of their functions are less well understood than in the case of miR-122 [31]. miR-122 is a key regulator of cholesterol and fatty-acid metabolism in the liver [32]. Therefore, it is likely that changes in the levels of miR-122 will predict not only liver damage but also the biological effects of that damage, such as abnormalities in fat metabolism. In addition, miR-122 has also been shown to be biomarkers for drug-induced liver injury in mice, rats, and human [33–35].

First, we showed that serum levels of miR-122 and miR-192 in nSP70-treated mice were elevated 8 h after treatment (figures 1(A) and (D)), as were those of ALT and AST (figures 1(B) and (C)), and that the levels of miR-122

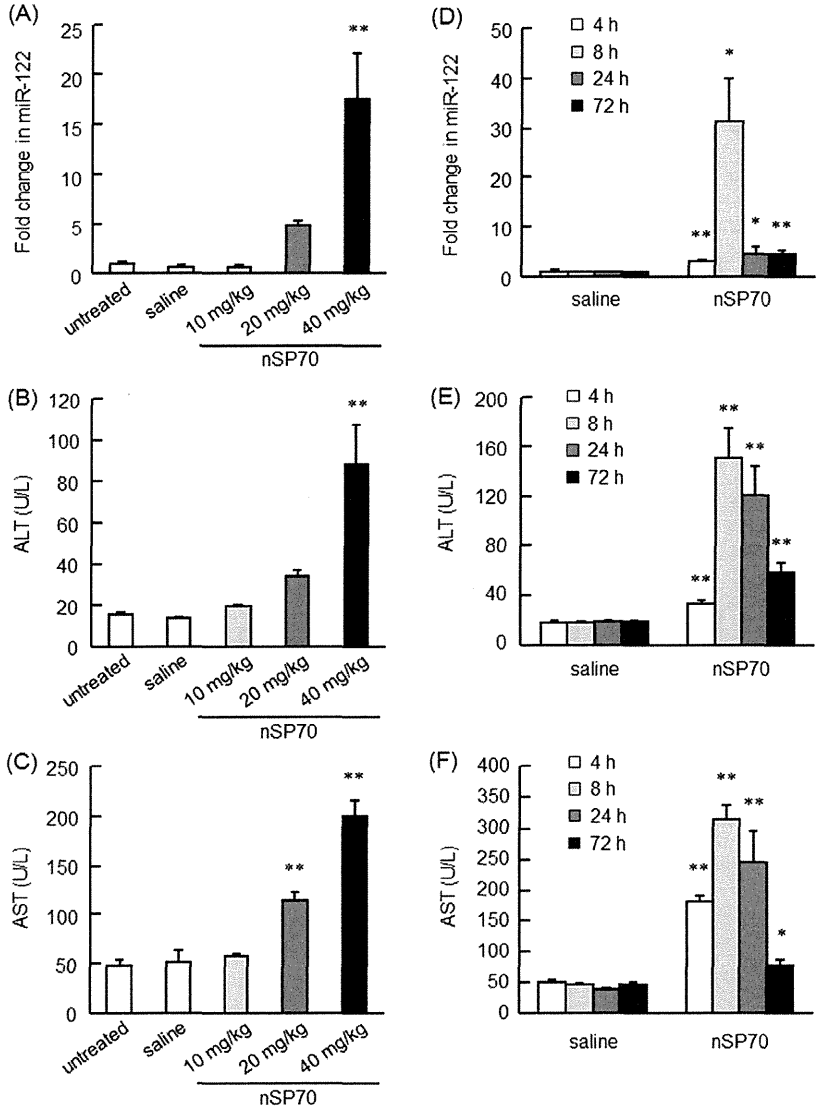


**Figure 2.** Serum levels of miR-122 after treatment with nSP70. BALB/c mice were intravenously treated with nSP70 at 10, 20, or 40 mg $kg^{-1}$. At 8 h after treatment with nSP70, the levels of (A) miR-122, (B) alanine aminotransferase (ALT), and (C) aspartate aminotransferase (AST) were analyzed. In addition, at 4, 8, 24, and 72 h after treatment with nSP70 at 40 mg $kg^{-1}$, the levels of (D) miR-122, (E) ALT, and (F) AST were examined. Data are presented as means ± SEM ($n = 5$ or 6; $^{*}P < 0.05$, $^{**}P < 0.01$ versus value for saline-treated group and untreated group by ANOVA).

were much higher than those of miR-192. We considered that this was because miR-122 accounts for 70% of all liver miRNA. By contrast, the serum levels of miR-194 in nSP70-treated mice did not differ significantly from those in untreated or saline-treated mice (figure 1(E)). The expression of miR-194 may change markedly with time; because we analyzed this expression only at 8 h after treatment, further time-course studies are needed before this miRNA can be discarded as a biomarker.

The serum levels of ALT and AST in mice treated with nSP70 at 40 mg $kg^{-1}$ were beyond the physiological range, at about 4 times the values in untreated or saline-treated mice. In contrast, the serum level of miR-122 in nSP70-treated mice was about 15 times that in untreated or saline-treated mice (figures 2(A)–(C)). This suggests that miR-122 may be a more sensitive biomarker than the currently used ALT and AST in detecting liver damage induced by nSP70. In addition, as shown in figures 2(A)–(C), we evaluated the dose-dependent expression of miR-122 only at 8 h after treatment with nSP70, and we showed that the pattern of expression of miR-122 was almost the same as that of ALT and AST. In another study, injection of acetaminophen did not cause serum ALT elevation at 1 h, although obvious increases in miR-122 and miR-192 levels were already observable [36]. Therefore, evaluation at time points earlier than 8 h after nSP70 injection with lower doses could reveal the possibility that miR-122 is a more sensitive predictor of nSP70-induced liver damage than ALT and AST.

As shown in figures 2(D)–(F), the serum levels of ALT and AST in mice treated with nSP70 at 24 h showed significantly greater than those in saline-treated mice, while for miRNA-122, it dropped at 24 h to the same level as

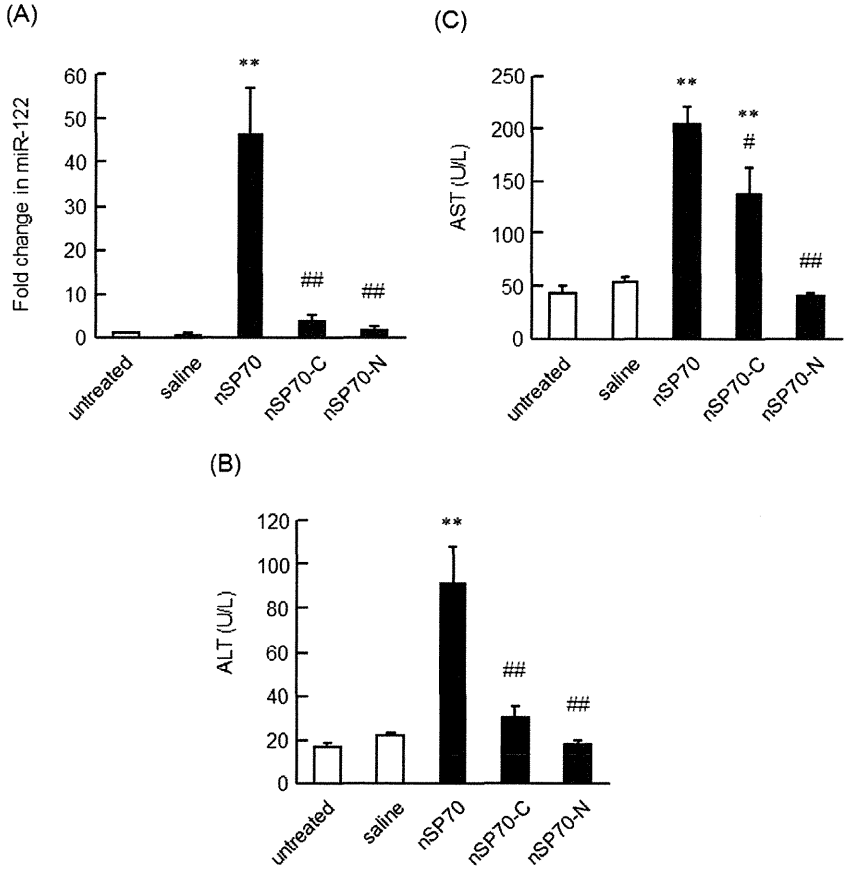


**Figure 3.** Responses of serum levels of miR-122 to treatment with surface-modified nSP70. BALB/c mice were intravenously treated with nSP70, nSP70-C, or nSP70-N at 40 mg $kg^{-1}$. Serum levels of (A) miR-122, (B) alanine aminotransferase (ALT), and (C) aspartate aminotransferase (AST) were measured 8 h after treatment. Data are presented as means ± SEM ($n = 5$ or 6; $^{**}P < 0.01$ versus value for saline-treated group and untreated group; $^{\#}P < 0.05$, $^{\#\#}P < 0.01$ versus value for nSP70-treated group by ANOVA).

72 h. In general, miRNAs are considered to be stable in the blood [37]. However, Yamaura *et al* showed that although miR-122 was stable in human plasma, it was unstable in rat plasma [38]. Therefore, although detailed information on the stability of mouse miR-122 is unavailable, it is possible that RNase action in the blood leads to a rapid decrease in miR-122 levels. Currently, there are two hypothetical pathways by which miRNAs can enter the circulation [39]. One is by direct leakage from cells, and the other is by release from cells via microvesicles. It is thought that direct secretion of miRNAs occurs in tissue damage or cell apoptosis [39]. We previously demonstrated that nSP70 administered via the tail vein was distributed mainly to the liver and induced cytotoxicity in primary hepatocytes isolated from nSP70-treated mice [7]. Taking these results together, it is conceivable that most miR-122 is leaked into the blood and degraded by RNase between 8 and 24 h after nSP70 treatment. On the other hand, the level of miR-122 in nSP70-treated mice showed significant increments compared to that of saline-treated mice over the time course of the experiment. Therefore, its change in expression over the full time course of the experiment was still useful for evaluating nSP70-induced liver damage. For these reasons, we consider that miR-122 is as useful as ALT and AST in evaluating nSP70-induced liver damage. However, because we cannot explain this in detail, we are now trying to investigate the mechanism involved.

Here, we evaluated the time course of miR-122 expression over only a short period of time after nSP70 treatment. However, considering that we are exposed to nanomaterials on a daily basis, there is a need to investigate the biological effects of long-term exposure to them. Recent reports have shown that long-term exposure to titanium dioxide nanomaterials in mice induces ROS production in the lung [40]. A nanomaterials safety-assessment system is required for the evaluation of not only acute effects but also chronic effects. Therefore, we intend to analyze nanomaterial-induced chronic biological effects by evaluating the long-term course of miRNA expression.

Although the levels of miR-122, ALT, and AST were lower in mice treated with modified nSP70 than in those treated with unmodified nSP70 (figure 3), the AST level in nSP70-C-treated mice was higher than that in untreated mice. It is possible that nSP70-C and nSP70-N is safer than nSP70, because we previously demonstrated that differences in the surface charge state or kind of functional group of nanomaterials lead to different biological effects and cell responses [41–43]. On the other hand, AST is abundant not only in the liver but also in the skeletal muscle, heart, and kidney. Taking these results together, we consider that the

increase in AST in nSP70-C-treated mice was attributable to damage to tissues other than the liver. We are now analyzing in detail the effects of nanomaterials by focusing on other tissues.

This study is just the first step in the development of a miRNA-based safety-assessment system for nanomaterials. We have shown here that miR-122 is almost as useful as ALT and AST as a biomarker for nanomaterials. Recent reports have shown that many miRNAs exist not only in blood but also in other body fluids such as urine or saliva [22, 23]. In light of these reports, we consider that miR-122 might have the potential to predict nSP70-induced liver damage non-invasively from analyses of urine or saliva. In addition, many tissue-specific miRNAs other than miR-122 have been reported [44]. Therefore, to develop more specific or more sensitive biomarkers than the established system, there is a strong need for comprehensive analyses of the miRNAs associated with various tissues, such as brain and pancreas, for which we do not have enough useful biomarkers. Considering that miRNAs regulate the expression of the mRNAs involved in protein translation, identifying the changes that occur in miRNA expression upon exposure to nanomaterials will enable us to predict the biological effects of these materials. We are now trying comprehensively to explore those miRNAs that show changes in expression levels upon exposure to nanomaterials. We hope that these studies will help to establish a system for evaluating the safety and usefulness of nanomaterials.

## 5. Conclusions

We have revealed here that miR-122 and miR-192 may be useful biomarkers of liver damage induced by nSP70. miR-122, in particular, may be comparable to ALT and AST as a biomarker for this purpose.

## Acknowledgments

This study was supported, in part, by Grants-in-Aid for Scientific Research from the Ministry of Education, Culture, Sports, Science and Technology of Japan (MEXT) and from the Japan Society for the Promotion of Science (JSPS); and by the Knowledge Cluster Initiative (MEXT); by Health Labour Sciences Research Grants from the Ministry of Health, Labour and Welfare of Japan (MHLW); by a Global Environment Research Fund from the Ministry of the Environment; by Food Safety Commission, Japan; by the Cosmetology Research Foundation; by the Smoking Research Foundation; by the Research Foundation for Pharmaceutical Sciences; by the Japan Food Chemical Research Foundation; and by the Takeda Science Foundation.

## References

[1] Kaur I P and Agrawal R 2007 *Recent Pat. Drug Deliv. Formul.* **1** 171–82
[2] Cormode D P, Jarzyna P A, Mulder W J and Fayad Z A 2010 *Adv. Drug Deliv. Rev.* **62** 329–38
[3] Nel A, Xia T, Madler L and Li N 2006 *Science* **311** 622–7
[4] Donaldson K, Murphy F A, Duffin R and Poland C A 2010 *Part. Fibre Toxicol.* **7** 5
[5] Shvedova A A, Kagan V E and Fadeel B 2010 *Annu. Rev. Pharmacol. Toxicol.* **50** 63–88
[6] Poland C A *et al* 2008 *Nature Nanotechnol.* **3** 423–8
[7] Nabeshi H *et al* 2011 *Biomaterials* **32** 2713–24
[8] Yamashita K *et al* 2011 *Nature Nanotechnol.* **6** 321–8
[9] Nabeshi H *et al* 2011 *Part. Fibre Toxicol.* **8** 1
[10] Nabeshi H *et al* 2012 *Nanotechnology* **23** 045101
[11] Higashisaka K *et al* 2011 *Biomaterials* **32** 3–9
[12] Higashisaka K *et al* 2012 *Nanoscale Res. Lett.* **7** 555
[13] Nagano T *et al* 2012 *Pharmazie* **67** 958–9
[14] Schickel R, Boyerinas B, Park S M and Peter M E 2008 *Oncogene* **27** 5959–74
[15] Cordes K R and Srivastava D 2009 *Circ. Res.* **104** 724–32
[16] Esquela-Kerscher A and Slack F J 2006 *Nature Rev. Cancer* **6** 259–69
[17] Pauley K M, Cha S and Chan E K 2009 *J. Autoimmun.* **32** 189–94
[18] Kosaka N, Iguchi H and Ochiya T 2010 *Cancer Sci.* **101** 2087–92
[19] Brase J C, Wuttig D, Kuner R and Sultmann H 2010 *Mol. Cancer* **9** 306
[20] Lagos-Quintana M, Rauhut R, Yalcin A, Meyer J, Lendeckel W and Tuschl T 2002 *Curr. Biol.* **12** 735–9
[21] Aboobaker A A, Tomancak P, Patel N, Rubin G M and Lai E C 2005 *Proc. Natl Acad. Sci. USA* **102** 18017–22
[22] Michael A, Bajracharya S D, Yuen P S, Zhou H, Star R A, Illei G G and Alevizos I 2010 *Oral Dis.* **16** 34–8
[23] Hanke M, Hoefig K, Merz H, Feller A C, Kausch I, Jocham D, Warnecke J M and Sczakiel G 2010 *Urol. Oncol.* **28** 655–61
[24] Yamada Y *et al* 2011 *Cancer Sci.* **102** 522–9
[25] Halappanavar S, Jackson P, Williams A, Jensen K A, Hougaard K S, Vogel U, Yauk C L and Wallin H 2011 *Environ. Mol. Mutagen.* **52** 425–39
[26] Burklew C E, Ashlock J, Winfrey W B and Zhang B 2012 *PLoS One* **7** e34783
[27] Cortez M A and Calin G A 2009 *Exp. Opin. Biol. Ther.* **9** 703–11
[28] Knopp D, Tang D and Niessner R 2009 *Anal. Chim. Acta* **647** 14–30
[29] Peters R *et al* 2012 *ACS Nano* **6** 2441–51
[30] Hou J *et al* 2011 *Cancer Cell* **19** 232–43
[31] Meng Z, Fu X, Chen X, Zeng S, Tian Y, Jove R, Xu R and Huang W 2010 *Hepatology* **52** 2148–57
[32] Rotllan N and Fernandez-Hernando C 2012 *Cholesterol* **2012** 847849
[33] Wang K, Zhang S, Marzolf B, Troisch P, Brightman A, Hu Z, Hood L E and Galas D J 2009 *Proc. Natl Acad. Sci. USA* **106** 4402–7
[34] Starkey Lewis P J *et al* 2011 *Hepatology* **54** 1767–76
[35] Starckx S *et al* 2013 *Toxicol. Pathol.* **41** 795–804
[36] Shi Q, Yang X and Mendrick D L 2013 *Biomark. Med.* **7** 307–15
[37] Gilad S *et al* 2008 *PLoS One* **3** e3148
[38] Yamaura Y, Nakajima M, Takagi S, Fukami T, Tsuneyama K and Yokoi T 2012 *PLoS One* **7** e30250
[39] Zen K and Zhang C Y 2012 *Med. Res. Rev.* **32** 326–48
[40] Sun Q *et al* 2012 *J. Biomed. Mater. Res.* A **100** 2554–62
[41] Nabeshi H *et al* 2011 *Nanoscale Res. Lett.* **6** 93
[42] Morishige T *et al* 2012 *Arch. Toxicol.* **86** 1297–307
[43] Yoshida T *et al* 2012 *Biochem. Biophys. Res. Commun.* **427** 748–52
[44] Laterza O F *et al* 2009 *Clin. Chem.* **55** 1977–83

European Journal of Pharmaceutical Sciences xxx (2013) xxx–xxx

Contents lists available at ScienceDirect

European Journal of Pharmaceutical Sciences

journal homepage: www.elsevier.com/locate/ejps

# Tissue distribution and safety evaluation of a claudin-targeting molecule, the C-terminal fragment of *Clostridium perfringens* enterotoxin

Xiangru Li, Rie Saeki, Akihiro Watari, Kiyohito Yagi, Masuo Kondoh *

*Laboratory of Bio-Functional Molecular Chemistry, Graduate School of Pharmaceutical Sciences, Osaka University, Suita, Osaka 565-0871, Japan*

ARTICLE INFO

*Article history:*
Received 2 April 2013
Received in revised form 25 October 2013
Accepted 25 October 2013
Available online xxxx

*Keywords:*
Claudin
*Clostridium perfringens* enterotoxin
Kidney
Liver
Tissue distribution

ABSTRACT

We previously found that claudin (CL) is a potent target for cancer therapy using a CL-3 and -4-targeting molecule, namely the C-terminal fragment of *Clostridium perfringens* enterotoxin (C-CPE). Although CL-3 and -4 are expressed in various normal tissues, the safety of this CL-targeting strategy has never been investigated. Here, we evaluated the tissue distribution of C-CPE in mice. Ten minutes after intravenous injection into mice, C-CPE was distributed to the liver and kidney (24.0% and 9.5% of the injected dose, respectively). The hepatic level gradually fell to 3.2% of the injected dose by 3 h post-injection, whereas the renal C-CPE level gradually rose to 46.5% of the injected dose by 6 h post-injection and then decreased. A C-CPE mutant protein lacking the ability to bind CL accumulated in the liver to a much lesser extent (2.0% of the dose at 10 min post-injection) than did C-CPE, but its renal profile was similar to that of C-CPE. To investigate the acute toxicity of CL-targeted toxin, we intravenously administered C-CPE-fused protein synthesis inhibitory factor to mice. The CL-targeted toxin dose-dependently increased the levels of serum biomarkers of liver injury, but not of kidney injury. Histological examination confirmed that injection of CL-targeted toxin injured the liver but not the kidney. These results indicate that potential adverse hepatic effects should be considered in C-CPE-based cancer therapy.



## 1. Introduction

Most lethal cancers are derived from epithelial tissues (Jemal et al., 2008), and many therapeutic strategies targeting such cancers have been developed. Selective delivery of anti-cancer agents to cancer cells is a popular anti-cancer strategy (Adair et al., 2012; Yewale et al., 2013). Many membrane proteins that are present at much higher levels in cancer cells than in normal cells have been identified. Antibodies have recently become available as anti-cancer drugs targeting breast cancer (pertuzumab, directed against human epidermal growth factor receptor-2) and colon cancer (panitumumab, directed against epidermal growth factor receptor) (Dent et al., 2013; Zouhairi et al., 2011).

Normal epithelial cells develop complex intercellular tight junctions (TJs) that prevent the free movement of solutes across epithelial cell sheets and of membrane proteins and lipids between apical and basolateral membranes (Furuse and Tsukita, 2006; Rodriguez-Boulan and Nelson, 1989; Vermeer et al., 2003). In contrast, TJ functionality is frequently abnormal in transformed epithelial cells. As a result, cellular polarity and intercellular contact are often lost, both in the early stages of carcinogenesis and in advanced tumors (Wodarz and Nathke, 2007). Such findings indicate that the membrane proteins of TJs, which are difficult to access in normal epithelia but are exposed in malignant cells, may be candidate targets for cancer therapy.

Freeze-fracture replica electron microscopy has shown that TJs present as a series of continuous, anastomotic, intramembranous particulate strands, or fibrils (Farquhar and Palade, 1963; Staehelin, 1973). The TJ-containing strands are composed of both intracellular and integral membrane proteins, including claudin (CL) (Anderson and Van Itallie, 2009). CL comprises a tetraspan protein family with 27 members (Mineta et al., 2011). Interestingly, the expression of CL-3 or -4, or both, is increased in breast, gastric, intestinal, ovarian, pancreatic, and prostatic carcinomas (Singh et al., 2010; Tsukita et al., 2008; Turksen and Troy, 2011).

*Clostridium perfringens* enterotoxin (CPE) causes food poisoning in humans (McClane and Chakrabarti, 2004). CL-3 and CL-4 serve as receptors for CPE, and CPE is cytotoxic to cells expressing these CLs (Long et al., 2001; Sonoda et al., 1999). Intratumoral administration of CPE attenuates pancreatic tumor growth, and intraperitoneal administration of CPE inhibits ovarian tumor growth

*Abbreviations:* ALT, alanine aminotransferase; AST, aspartate aminotransferase; BSA, bovine serum albumin; BUN, blood urea nitrogen; CL, claudin; CPE, *Clostridium perfringens* enterotoxin; C-CPE, C-terminal fragment of CPE; FACS, fluorescence-activated cell sorter; PBS, phosphate-buffered saline; PSIF, protein synthesis inhibitory factor; TJ, tight junction.

* Corresponding author. Tel.: +81 6 6879 8196; fax: +81 6 6879 8199.
*E-mail address:* masuo@phs.osaka-u.ac.jp (M. Kondoh).

0928-0987/$ - see front matter © 2013 Published by Elsevier B.V.
http://dx.doi.org/10.1016/j.ejps.2013.10.018

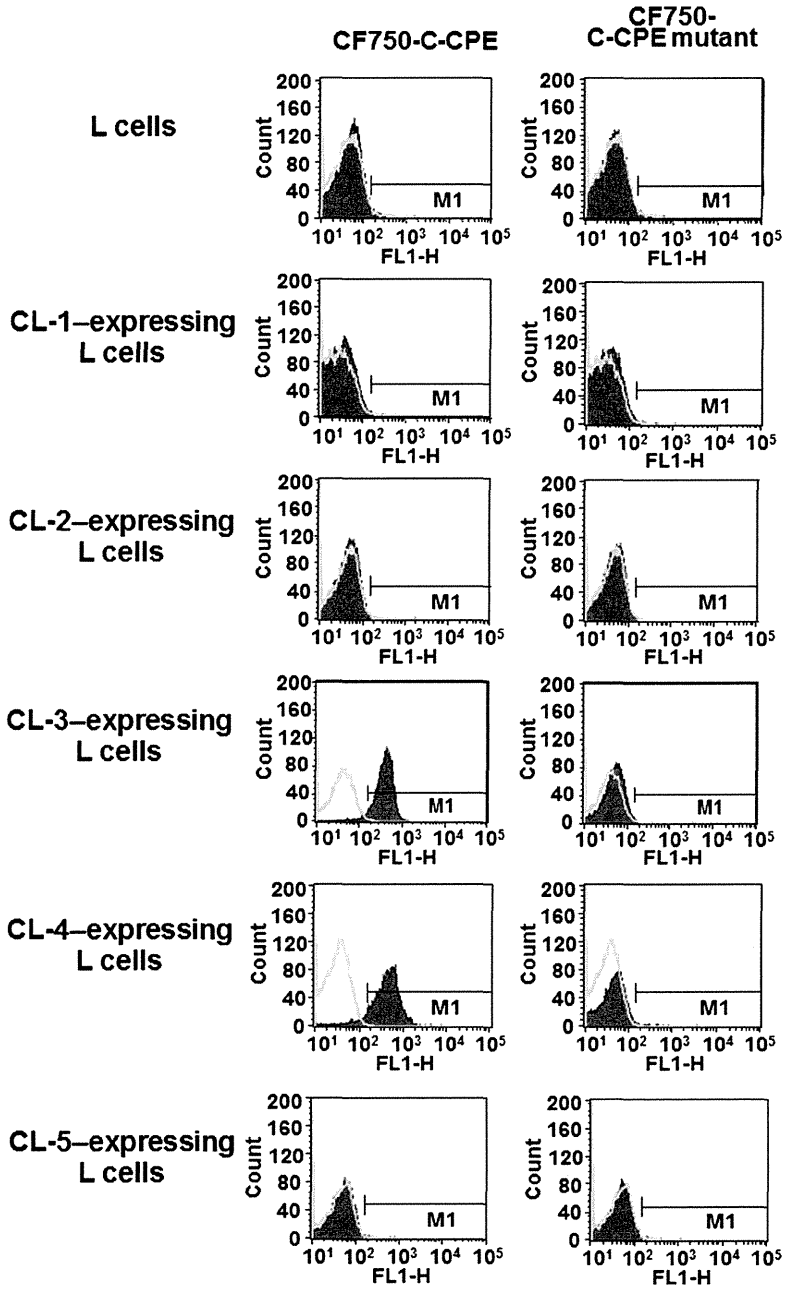


**Fig. 1.** Flow cytometric analysis of the interaction of claudins (CLs) with the CF750-labeled C-terminal fragment of *Clostridium perfringens* enterotoxin (C-CPE). Mouse fibroblast L cells were incubated with 10 μg/ml CF750-labeled C-CPE or a mutant form of C-CPE (also labeled with CF750) for 1 h and then subjected to fluorescence-activated cell sorter analysis as described in the Materials and Methods. Unfilled curves show the results obtained when cells were not treated with C-CPE proteins. Filled curves show data from C-CPE-treated cells. FL1-H indicates fluorescent intensity and M1 indicates C-CPE-bound cells.

(Michl et al., 2001; Santin et al., 2005). Moreover, the C-terminal fragment of CPE (C-CPE) is a ligand of CL-3 and CL-4 (Sonoda et al., 1999). We previously prepared a CL-targeting cytotoxic molecule via fusion of C-CPE and a protein synthesis inhibitory factor (PSIF) derived from *Pseudomonas* exotoxin (Ebihara et al., 2006). We found that intratumoral or intravenous administration of C-CPE-fused PSIF attenuated the growth of murine breast cancer cells (Saeki et al., 2009, 2010). Thus, drugs that include all or part of CPE may be useful for targeting CLs in cancer therapy.

CLs are expressed throughout the body. Evaluation of the possible adverse effects of CL-targeting molecules is critical if the CPE technology described above is to be used for cancer therapy. However, no such hazard assessment has been performed to date. Here, we investigated the tissue distribution of C-CPE and the tissue injury caused by C-CPE-fused PSIF.

## 2. Materials and methods

### 2.1. Cell cultures

Mouse fibroblast L cells expressing mouse CL-1, CL-2, CL-3, CL-4, or CL-5 were kindly provided by Dr. S. Tsukita (Kyoto University). Cells were cultured in Eagle's minimum essential medium with 10% (v/v) fetal calf serum and 500 μg/ml G418 at 37 °C under a 5% (v/v) $CO_2$ atmosphere.

Please cite this article in press as: Li, X., et al. Tissue distribution and safety evaluation of a claudin-targeting molecule, the C-terminal fragment of *Clostridium perfringens* enterotoxin. Eur. J. Pharm. Sci. (2013), http://dx.doi.org/10.1016/j.ejps.2013.10.018

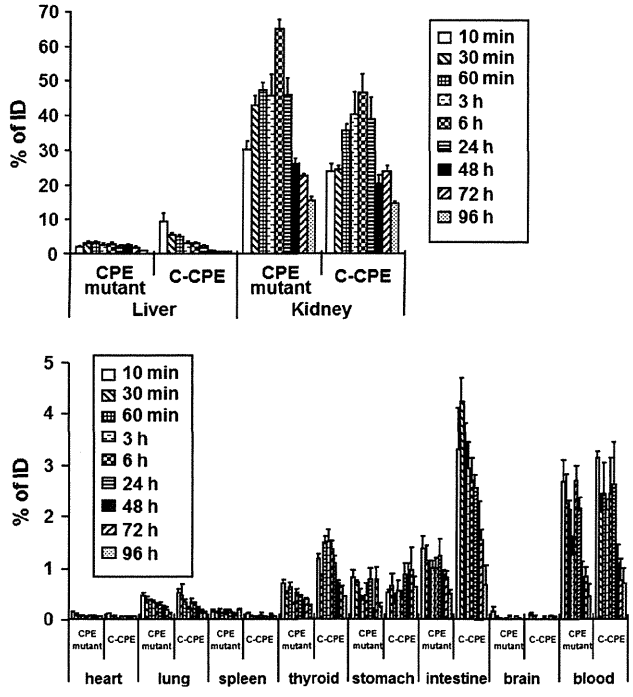


**Fig. 2.** *In vivo* distribution of the CF750-labeled C-terminal fragment of *Clostridium perfringens* enterotoxin (C-CPE). Mice were intravenously injected with 2 μg/mouse CF750-labeled C-CPE or a CF750-labeled C-CPE mutant. Tissues were removed at the indicated times after injection and the intensity of fluorescence of each tissue was measured as described in the Materials and Methods. Tissue C-CPE levels were calculated as percentages of injected doses. Data are means ± SEM ($n = 5$). ID, injected dose.

### 2.2. Preparation of C-CPE and C-CPE mutant protein

C-CPE, and a mutant form thereof, in which Ala was substituted with Tyr and Leu at positions 306 and 315, were prepared as described previously (Takahashi et al., 2008). Briefly, recombinant plasmids derived from pET-16b, pET-C-CPE encoding histidine (His)-tagged C-CPE, or a pET-C-CPE mutant encoding His-tagged C-CPE mutant protein, were transduced into *Escherichia coli* strain BL21 (DE3) (Novagen, Darmstadt, Germany), and production of recombinant proteins was induced by adding isopropyl-β-D-thiogalactopyranoside. Harvested cells were lysed in buffer A (10 mM Tris–HCl [pH 8.0], 400 mM NaCl, 5 mM $MgCl_2$, 0.1 mM phenylmethylsulfonyl fluoride, 1 mM 2-mercaptoethanol, and 10% [v/v] glycerol). Each lysate was applied to a HiTrap chelating HP column (GE Healthcare, Chalfont St Giles, Buckinghamshire, UK), and the recombinant protein was eluted with buffer A containing imidazole. This buffer was exchanged for phosphate-buffered saline (PBS) by using a PD-10 column (GE Healthcare), and the purified proteins dissolved in PBS were stored at −80 °C until use. The purity of the recombinant proteins was confirmed by sodium dodecyl sulfate–polyacrylamide gel electrophoresis followed by staining with Coomassie brilliant blue. Protein concentrations were quantified with a BCA protein assay kit, using bovine serum albumin (BSA) as a standard (Pierce Chemicals, Rockford, IL).

### 2.3. Animals

Female BALB/c mice (6–8 weeks of age) were purchased from SLC, Inc. (Shizuoka, Japan). Mice were housed at 23 ± 1.5 °C with a 12-h light/12-h dark cycle and had free access to water and commercial chow (Type MF; Oriental Yeast, Tokyo, Japan). Mice were allowed to adapt to these conditions for at least 1 week after arrival. All animal experiments adhered to the ethical guidelines of the Graduate School of Pharmaceutical Sciences, Osaka University.

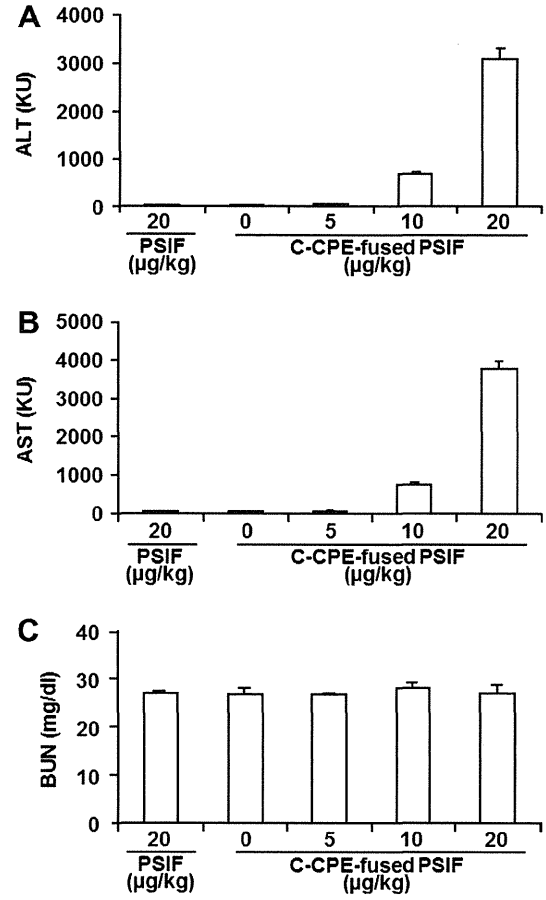


**Fig. 3.** Serum markers of liver and kidney injury in mice injected with protein synthesis inhibitory factor (PSIF) fused to the C-terminal fragment of *Clostridium perfringens* enterotoxin (C-CPE). Mice were intravenously injected with PSIF at 2 μg/kg or C-CPE-fused PSIF at 0, 5, 10, or 20 μg/kg. Twenty-four hours later, serum ALT (A), AST (B), and BUN (C) levels were measured as described in the Materials and Methods. Data are presented as means ± SEM ($n = 5$).

### 2.4. Preparation of CF750-labeled C-CPE proteins

C-CPE and the mutant form of the protein were labeled with the fluorescent dye CF750 by using a XenoLight CF750 rapid antibody-labeling kit (Caliper Life Sciences, Inc., Hopkinton, MA), in accordance with the manufacturer's instructions. The concentrations of labeled C-CPEs were calculated according to the manufacturer's protocol by using the following equation: Concentration (mg/ml) = {[absorbance at 280 nm minus (absorbance at 755 nm × 0.3)]/0.46} × dilution factor.

### 2.5. Fluorescence-activated cell sorter (FACS) analysis

L-cells expressing various CLs were harvested with trypsin and suspended in PBS. The cells were incubated with C-CPE or the mutant form of C-CPE for 1 h at 4 °C; this was followed by incubation with anti-His-tag antibody. Cells were next incubated with fluorescein-labeled secondary antibody, and cells that bound the test proteins were detected and analyzed by flow cytometry (FACScalibur, Becton Dickinson, Franklin Lakes, NJ).

### 2.6. Tissue distribution of injected proteins

C-CPE, or the mutant form thereof, labeled with CF750, was intravenously injected into mice at 2 μg/100 μl of PBS per mouse. Mice were sacrificed 10 min, 30 min, 60 min, 3 h, 6 h, 24 h, 48 h,

Please cite this article in press as: Li, X., et al. Tissue distribution and safety evaluation of a claudin-targeting molecule, the C-terminal fragment of *Clostridium perfringens* enterotoxin. Eur. J. Pharm. Sci. (2013), http://dx.doi.org/10.1016/j.ejps.2013.10.018

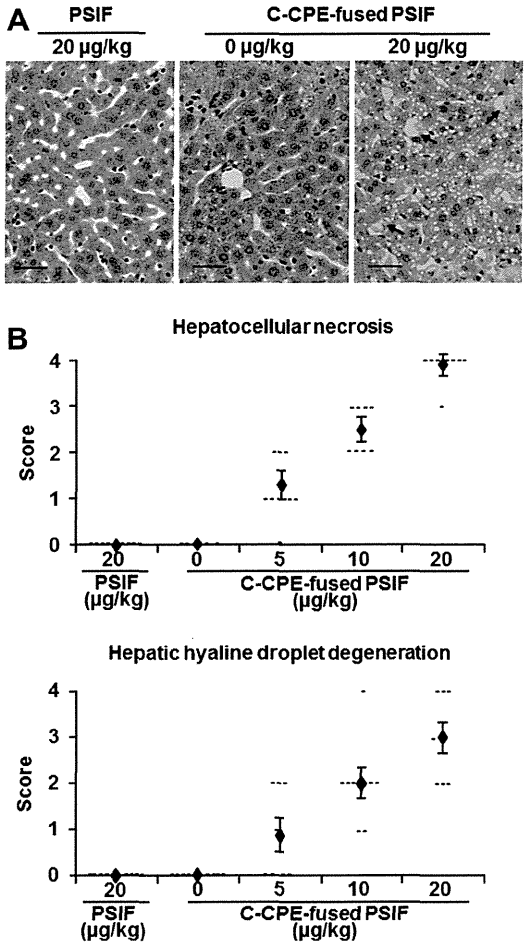


**Fig. 4.** Histological analysis of the livers of mice injected with protein synthesis inhibitory factor (PSIF) fused to the C-terminal fragment of *Clostridium perfringens* enterotoxin (C-CPE). Mice were intravenously injected with PSIF at 20 μg/kg or C-CPE-fused PSIF at 0, 5, 10, or 20 μg/kg ($n = 7$ or 8). Twenty-four hours later, the livers were removed and fixed in formaldehyde. Sections were stained with hematoxylin–eosin and examined microscopically for pathology. A representative micrograph is shown in panel A; arrows indicate regions of injury (scale bar, 60 μm). The extents of hepatocellular necrosis and hepatic hyaline droplet degeneration were scored (panel B) as follows: 0, none; 1, very mild; 2, mild; 3, moderate; or 4, high. Each horizontal dash represents the score of one sample. Data are means ± SEM ($n = 7$ or 8).

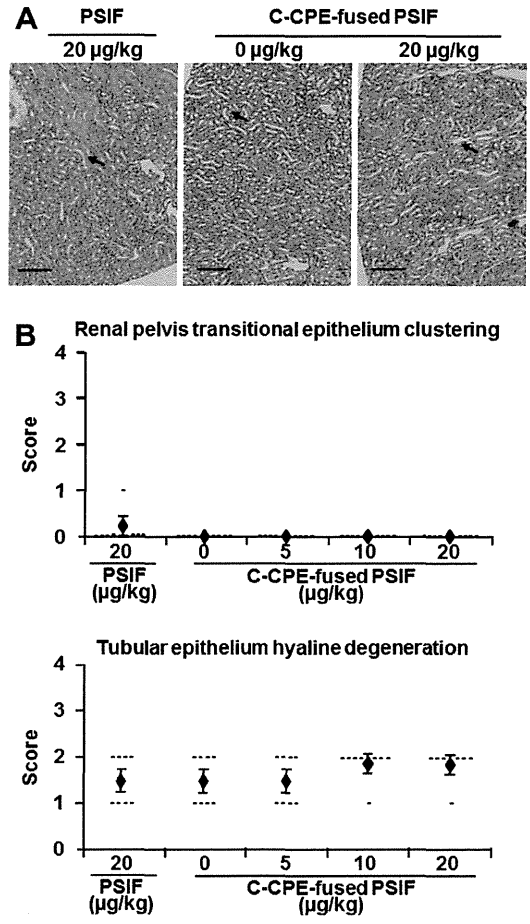


**Fig. 5.** Histological analysis of the kidneys of mice injected with protein synthesis inhibitory factor (PSIF) fused to the C-terminal fragment of *Clostridium perfringens* enterotoxin (C-CPE). Mice were intravenously injected with PSIF at 20 μg/kg or C-CPE-fused PSIF at 0, 5, 10, or 20 μg/kg ($n = 7$ or 8). Twenty-four hours later, the kidneys were removed and fixed in formaldehyde. Sections were stained with hematoxylin-eosin and examined microscopically for pathology. A representative micrograph is shown in panel A; arrows indicate regions of injury (scale bar, 240 μm). The extent of clustering of the renal pelvis transitional epithelium and the level of hyaline degeneration of the tubular epithelium were scored (panel B) as follows: 0, none; 1, very mild; 2, mild; 3, moderate; or 4, high. Each horizontal dash represents the score of one sample. Data are means ± SEM ($n = 7$ or 8).

72 h, or 96 h later. The blood, heart, lung, liver, spleen, kidney, thyroid, stomach, intestine, and brain were excised from each mouse. The blood and organs from each mouse were placed side-by-side and imaged by using a Maestro EX *in vivo* imaging system, version 2.10.0 (Cambridge Research & Instrumentation Inc., Woburn, MA). The imaging system was equipped with an excitation filter (wavelength 229–684 nm). Fluorescence was detected by a CCD camera equipped with a C-mount lens and a long-pass emission filter (745 nm). Spectral data "cubes" were created by acquisition of a series of images obtained by using different wavelengths. In such cubes, each pixel is associated with a spectrum. Maestro software can be used to analyze these data; any autofluorescence can be identified, separated from the CF750 fluorescence, and removed. The resulting signals (counts) from each tissue were used to evaluate C-CPE distributions. The levels of C-CPEs in each tissue, as percentages of injected doses, were calculated. Total blood volume was calculated as 8% of body weight.

### 2.7. Preparation of C-CPE-fused PSIF

PSIF and C-CPE-fused PSIF were prepared as described previously (Saeki et al., 2009). In brief, plasmid pET-PSIF or pET-C-CPE-PSIF was transduced into *E. coli* BL21 (DE3) and recombinant protein production was induced by adding 0.25 mM isopropyl-β-D-thiogalactopyranoside. Harvested cells were lysed in buffer A. The lysates were centrifuged and the supernatants applied to Hi-Trap chelating HP columns. Recombinant proteins were eluted with imidazole-containing buffer A. This buffer was exchanged for PBS by using a PD-10 column, and the purified protein solutions were stored at −80 °C until use. Protein concentrations were quantified with a BCA protein assay kit, using BSA as a standard.

### 2.8. Biochemical assays

Mice were intravenously injected with 100 μl of C-CPE-fused PSIF at 0, 5, 10, or 20 μg/kg, or with 100 μl of PSIF at 20 μg/kg.

Please cite this article in press as: Li, X., et al. Tissue distribution and safety evaluation of a claudin-targeting molecule, the C-terminal fragment of *Clostridium perfringens* enterotoxin. Eur. J. Pharm. Sci. (2013), http://dx.doi.org/10.1016/j.ejps.2013.10.018

Twenty-four hours after the injection, serum levels of alanine aminotransferase (ALT), aspartate aminotransferase (AST), and blood urea nitrogen (BUN) were measured with commercial kits (Transaminase-CII kit [ALT, AST] and Blood Urea Nitrogen-B Test [BUN]; Wako Pure Chemicals, Osaka, Japan).

### 2.9. Histological analysis

Livers and kidneys were removed and fixed in 4% (v/v) paraformaldehyde. Thin sections were stained with hematoxylin and eosin before histological observation. The extent of injury was scored as 0, none; 1, very mild; 2, mild; 3, moderate; or 4, high.

## 3. Results

### 3.1. Tissue distribution of the CL-3/-4-binding agent C-CPE

The fluorescent dye CF750 was conjugated to the CL-3/-4-binding agent C-CPE to allow the tissue distribution of C-CPE to be monitored. FACS analysis revealed that CF750-labeled C-CPE bound to CL-3- or CL-4-expressing L-cells but not to mock-, CL-1-, CL-2-, or CL-5-expressing L cells (Fig. 1). Thus, labeling of C-CPE with CF750 did not affect the binding profile of C-CPE to CLs. As a control, we also prepared a CF750-labeled C-CPE mutant protein lacking CL-binding activity; Ala was substituted for the wild-type Tyr306 and Leu315 in the mutant protein (Takahashi et al., 2008). The C-CPE mutant did not bind to the cells (Fig. 1).

C-CPE was evident in the kidney (24.0% of the injected dose), liver (9.5%), intestine (3.3%), and thyroid (1.2%) 10 min after intravenous injection (Fig. 2). The levels of C-CPE in the liver, intestine, and thyroid gradually fell thereafter, to 0.4%, 0.7%, and 0.4% of the injected dose, respectively, at 96 h post-injection. In contrast, the level of C-CPE in the kidney increased to 46.5% of the injected dose 6 h after injection and only then began to fall, reaching 14.4% of the injected dose 96 h post-injection. The control C-CPE mutant protein became distributed in the liver (2.0% of the injected dose), intestine (1.4%), and thyroid (0.7%) at levels much lower than those of C-CPE at 10 min post-injection, but the levels of the mutant protein in the kidney were comparable to those of C-CPE (Fig. 2). Therefore, the liver may be a major target tissue of CL-3/-4-binding protein, whereas accumulation in the kidney may not be associated with CL-3/-4 targeting.

### 3.2. Effects of a CL-3/-4-targeting toxin on the liver and kidney

We previously found that tail vein injection of C-CPE-fused PSIF at 5 μg/kg every 2 days for 14 days had anti-tumor activity without hepatotoxicity or nephrotoxicity (Saeki et al., 2010). Here, to evaluate the acute toxicity of a CL-targeting toxin to the liver and kidney, we intravenously injected mice with C-CPE-fused PSIF, or control PSIF alone, and measured biochemical markers of liver (ALT and AST) and kidney (BUN) injury 24-h later. Injection of PSIF alone (20 μg/kg) did not increase serum ALT, AST, or BUN levels. Injection of C-CPE-fused PSIF at doses of 0, 5, 10, and 20 μg/kg increased serum ALT and AST levels in a dose-dependent manner (ALT: 21, 49, 668, and 3053 karmen unit (KU) respectively; AST: 49, 68, 764, and 3781 KU, respectively) (Fig. 3A and B). In contrast, injection of C-CPE-fused PSIF, even at 20 μg/kg, did not increase the serum BUN level (Fig. 3C). Injection of C-CPE-fused PSIF at 10 or 20 μg/kg, but not at 5 μg/kg, caused body weight loss and reduced mobility (data not shown). Histologically, C-CPE-fused PSIF caused hepatocellular necrosis and hyaline droplet degeneration (Fig. 4A, B). Although injection of C-CPE-fused PSIF caused slight hyaline degeneration of the tubular epithelium of the kidney, injection of PSIF alone had a similar effect (Fig. 5A and B). Therefore, the low-level kidney injury evident after administration of C-CPE-fused PSIF may not have been associated with the targeting of CLs.

## 4. Discussion

CPE was the first CL-3/-4-targeting toxin to be described (Fujita et al., 2000; Sonoda et al., 1999), and C-CPE-fused PSIF was the second (Ebihara et al., 2006; Saeki et al., 2009). A series of studies using CPE and C-CPE have provided proof-of-concept that CL targeting is a strategy for cancer therapy (Long et al., 2001; Michl et al., 2001; Neesse et al., 2013; Saeki et al., 2009, 2010; Santin et al., 2005). However, because CL-3 and CL-4 are expressed in various normal tissues (Morita et al., 1999; Turksen and Troy, 2011), risk assessment of CL-targeting molecules is needed when CPE technology is applied to cancer therapy. Here, we found that systemic injection of a C-CPE-fused toxin resulted in acute hepatic, but not renal, toxicity 24 h after injection in mice.

After injection, C-CPE accumulates to the greatest extent in the liver and kidney. The expression profiles of CL-3 and CL-4 differ in these two tissues. In the liver, CL-3 is locally expressed in the lateral membranes of all lobular hepatocytes (Rahner et al., 2001); the liver does not express CL-4 (Morita et al., 1999). In contrast, CL-3 and CL-4 are locally expressed, in the kidney, in the lateral membranes of epithelial-cell sheets of the loop of Henle, the distal tubule, and the collecting duct (Balkovetz, 2009). Epithelial cells of the kidney form a boundary between the inner and outer regions, and the TJs act as barriers, preventing free movement of solutes across epithelial sheets (Hou et al., 2010; Milatz et al., 2010). In contrast, hepatocytes do not have a barrier function, with the exception of those located in the canaliculi. Therefore, CL-targeting molecules can access CL-3 in parts of the liver other than the canaliculi, but not CL-3 and CL-4 in the renal epithelium. C-CPE-fused PSIF must be taken up by cells if the drug is to be cytotoxic, because inhibition of ribosomal elongation factor-2 by the PSIF domain is the cause of cell death (Ebihara et al., 2006; Kreitman and Pastan, 2006; Ogata et al., 1990).

Here, we found that hepatic accumulation of a toxin fused to C-CPE could have adverse effects if C-CPE-based cancer therapy were prescribed. C-CPE binds to both CL-3 and CL-4. Levels of CL-4 are increased more frequently than those of CL-3 in cancers such as breast, gastric, intestinal, ovarian, pancreatic, and prostate carcinomas (Singh et al., 2010; Tsukita et al., 2008; Turksen and Troy, 2011). Thus, development of a C-CPE mutant that binds to CL-4 but not to CL-3 may be useful in cancer therapy. We previously found that modulation of the electrostatic profile of the C-CPE surface can change the CL-binding profile (Takahashi et al., 2012). Veshnyakova et al. (2012) showed that the C-CPE residues, Leu223, Asp225, and Arg227, were involved in binding to CL-3, whereas Leu254, Ser256, Ile258, and Asp284 were involved in binding to CL-4. Manipulation of the electrostatic surface and the C-CPE residues may allow us to develop a C-CPE mutant that binds specifically to CL-4.

## Acknowledgements

We thank the staff of our laboratory for their useful comments and discussion. This work was supported by Grants-in-Aids for Scientific Research from the Ministry of Education, Culture, Sports, Science, and Technology of Japan (Nos. 21689006 and 24390042); by a Health and Labor Sciences Research Grant from the Ministry of Health, Labour, and Welfare of Japan; by the Takeda Science Foundation; by the Nakatomi Foundation; and by the Platform for Drug Discovery, Informatics, and Structural Life Science of the Ministry of Education, Culture, Sports, Science, and Technology, Japan.

Please cite this article in press as: Li, X., et al. Tissue distribution and safety evaluation of a claudin-targeting molecule, the C-terminal fragment of *Clostridium perfringens* enterotoxin. Eur. J. Pharm. Sci. (2013), http://dx.doi.org/10.1016/j.ejps.2013.10.018

## References

Adair, J.R., Howard, P.W., Hartley, J.A., Williams, D.G., Chester, K.A., 2012. Antibody-drug conjugates – a perfect synergy. Expert. Opin. Biol. Ther. 12, 1191–1206.

Anderson, J.M., Van Itallie, C.M., 2009. Physiology and function of the tight junction. Cold Spring Harbor Perspect. Biol. 1, a002584.

Balkovetz, D.F., 2009. Tight junction claudins and the kidney in sickness and in health. Biochim. Biophys. Acta 1788, 858–863.

Dent, S., Oyan, B., Honig, A., Mano, M., Howell, S., 2013. HER2-targeted therapy in breast cancer: a systematic review of neoadjuvant trials. Cancer Treat. Rev. 39, 622–631.

Ebihara, C., Kondoh, M., Hasuike, N., Harada, M., Mizuguchi, H., Horiguchi, Y., Fujii, M., Watanabe, Y., 2006. Preparation of a claudin-targeting molecule using a C-terminal fragment of *Clostridium perfringens* enterotoxin. J. Pharmacol. Exp. Ther. 316, 255–260.

Farquhar, M.G., Palade, G.E., 1963. Junctional complexes in various epithelia. J. Cell Biol. 17, 375–412.

Fujita, K., Katahira, J., Horiguchi, Y., Sonoda, N., Furuse, M., Tsukita, S., 2000. *Clostridium perfringens* enterotoxin binds to the second extracellular loop of claudin-3, a tight junction integral membrane protein. FEBS Lett. 476, 258–261.

Furuse, M., Tsukita, S., 2006. Claudins in occluding junctions of humans and flies. Trends Cell Biol. 16, 181–188.

Hou, J., Renigunta, A., Yang, J., Waldegger, S., 2010. Claudin-4 forms paracellular chloride channel in the kidney and requires claudin-8 for tight junction localization. Proc. Natl. Acad. Sci. USA 107, 18010–18015.

Jemal, A., Siegel, R., Ward, E., Hao, Y., Xu, J., Murray, T., Thun, M.J., 2008. Cancer statistics, 2008. CA Cancer J. Clin. 58, 71–96.

Kreitman, R.J., Pastan, I., 2006. Immunotoxins in the treatment of hematologic malignancies. Curr. Drug Targets 7, 1301–1311.

Long, H., Crean, C.D., Lee, W.H., Cummings, O.W., Gabig, T.G., 2001. Expression of *Clostridium perfringens* enterotoxin receptors claudin-3 and claudin-4 in prostate cancer epithelium. Cancer Res. 61, 7878–7881.

McClane, B.A., Chakrabarti, G., 2004. New insights into the cytotoxic mechanisms of *Clostridium perfringens* enterotoxin. Anaerobe 10, 107–114.

Michl, P., Buchholz, M., Rolke, M., Kunsch, S., Lohr, M., McClane, B., Tsukita, S., Leder, G., Adler, G., Gress, T.M., 2001. Claudin-4: a new target for pancreatic cancer treatment using *Clostridium perfringens* enterotoxin. Gastroenterology 121, 678–684.

Milatz, S., Krug, S.M., Rosenthal, R., Gunzel, D., Muller, D., Schulzke, J.D., Amasheh, S., Fromm, M., 2010. Claudin-3 acts as a sealing component of the tight junction for ions of either charge and uncharged solutes. Biochim. Biophys. Acta 1798, 2048–2057.

Mineta, K., Yamamoto, Y., Yamazaki, Y., Tanaka, H., Tada, Y., Saito, K., Tamura, A., Igarashi, M., Endo, T., Takeuchi, K., Tsukita, S., 2011. Predicted expansion of the claudin multigene family. FEBS Lett. 585, 606–612.

Morita, K., Furuse, M., Fujimoto, K., Tsukita, S., 1999. Claudin multigene family encoding four-transmembrane domain protein components of tight junction strands. Proc. Natl. Acad. Sci. USA 96, 511–516.

Neesse, A., Hahnenkamp, A., Griesmann, H., Buchholz, M., Hahn, S.A., Maghnouj, A., Fendrich, V., Ring, J., Sipos, B., Tuveson, D.A., Bremer, C., Gress, T.M., Michl, P., 2013. Claudin-4-targeted optical imaging detects pancreatic cancer and its precursor lesions. Gut 62, 1034–1043.

Ogata, M., Chaudhary, V.K., Pastan, I., FitzGerald, D.J., 1990. Processing of *Pseudomonas* exotoxin by a cellular protease results in the generation of a 37,000-Da toxin fragment that is translocated to the cytosol. J. Biol. Chem. 265, 20678–20685.

Rahner, C., Mitic, L.L., Anderson, J.M., 2001. Heterogeneity in expression and subcellular localization of claudins 2, 3, 4, and 5 in the rat liver, pancreas, and gut. Gastroenterology 120, 411–422.

Rodriguez-Boulan, E., Nelson, W.J., 1989. Morphogenesis of the polarized epithelial cell phenotype. Science 245, 718–725.

Saeki, R., Kondoh, M., Kakutani, H., Tsunoda, S., Mochizuki, Y., Hamakubo, T., Tsutsumi, Y., Horiguchi, Y., Yagi, K., 2009. A novel tumor-targeted therapy using a claudin-4-targeting molecule. Mol. Pharmacol. 76, 918–926.

Saeki, R., Kondoh, M., Kakutani, H., Matsuhisa, K., Takahashi, A., Suzuki, H., Kakamu, Y., Watari, A., Yagi, K., 2010. A claudin-targeting molecule as an inhibitor of tumor metastasis. J. Pharmacol. Exp. Ther. 334, 576–582.

Santin, A.D., Cane, S., Bellone, S., Palmieri, M., Siegel, E.R., Thomas, M., Roman, J.J., Burnett, A., Cannon, M.J., Pecorelli, S., 2005. Treatment of chemotherapy-resistant human ovarian cancer xenografts in C.B-17/SCID mice by intraperitoneal administration of *Clostridium perfringens* enterotoxin. Cancer Res. 65, 4334–4342.

Singh, A.B., Sharma, A., Dhawan, P., 2010. Claudin family of proteins and cancer: an overview. J. Oncol. 2010, 541957.

Sonoda, N., Furuse, M., Sasaki, H., Yonemura, S., Katahira, J., Horiguchi, Y., Tsukita, S., 1999. *Clostridium perfringens* enterotoxin fragment removes specific claudins from tight junction strands: evidence for direct involvement of claudins in tight junction barrier. J. Cell Biol. 147, 195–204.

Staehelin, L.A., 1973. Further observations on the fine structure of freeze-cleaved tight junctions. J. Cell Sci. 13, 763–786.

Takahashi, A., Komiya, E., Kakutani, H., Yoshida, T., Fujii, M., Horiguchi, Y., Mizuguchi, H., Tsutsumi, Y., Tsunoda, S., Koizumi, N., Isoda, K., Yagi, K., Watanabe, Y., Kondoh, M., 2008. Domain mapping of a claudin-4 modulator, the C-terminal region of C-terminal fragment of *Clostridium perfringens* enterotoxin, by site-directed mutagenesis. Biochem. Pharmacol. 75, 1639–1648.

Takahashi, A., Saito, Y., Kondoh, M., Matsushita, K., Krug, S.M., Suzuki, H., Tsujino, H., Li, X., Aoyama, H., Matsuhisa, K., Uno, T., Fromm, M., Hamakubo, T., Yagi, K., 2012. Creation and biochemical analysis of a broad-specific claudin binder. Biomaterials 33, 3464–3474.

Tsukita, S., Yamazaki, Y., Katsuno, T., Tamura, A., Tsukita, S., 2008. Tight junction-based epithelial microenvironment and cell proliferation. Oncogene 27, 6930–6938.

Turksen, K., Troy, T.C., 2011. Junctions gone bad: claudins and loss of the barrier in cancer. Biochim. Biophys. Acta 1816, 73–79.

Vermeer, P.D., Einwalter, L.A., Moninger, T.O., Rokhlina, T., Kern, J.A., Zabner, J., Welsh, M.J., 2003. Segregation of receptor and ligand regulates activation of epithelial growth factor receptor. Nature 422, 322–326.

Veshnyakova, A., Piontek, J., Protze, J., Waziri, N., Heise, I., Krause, G., 2012. Mechanism of *Clostridium perfringens* enterotoxin interaction with claudin-3/-4 protein suggests structural modifications of the toxin to target specific claudins. J. Biol. Chem. 287, 1698–1708.

Wodarz, A., Nathke, I., 2007. Cell polarity in development and cancer. Nat. Cell Biol. 9, 1016–1024.

Yewale, C., Baradia, D., Vhora, I., Misra, A., 2013. Proteins: emerging carrier for delivery of cancer therapeutics. Expert Opin. Drug Deliv. 10, 1429–1448.

Zouhairi, M., Charabaty, A., Pishvaian, M.J., 2011. Molecularly targeted therapy for metastatic colon cancer: proven treatments and promising new agents. Gastrointest. Cancer Res. 4, 15–21.

Please cite this article in press as: Li, X., et al. Tissue distribution and safety evaluation of a claudin-targeting molecule, the C-terminal fragment of *Clostridium perfringens* enterotoxin. Eur. J. Pharm. Sci. (2013), http://dx.doi.org/10.1016/j.ejps.2013.10.018